 

Selected Paper

# Highly Coplanar Polythiophenes with –C≡CR Side Chains: Self-Assembly, Linear and Nonlinear Optical Properties, and Piezochromism

**Takakazu Yamamoto,*[1] Takao Sato,[1] Takayuki Iijima,[1] Masahiro Abe,[1] Hiroki Fukumoto,[1] Take-aki Koizumi,[1] Motoaki Usui,[1] Yoshiyuki Nakamura,[1] Takehiko Yagi,[2] Hiroyuki Tajima,[2] Taku Okada,[2] Shintaro Sasaki,[3] Hideo Kishida,[4] Arao Nakamura,[4] Takashi Fukuda,[5] Akira Emoto,[5] Hirobumi Ushijima,[5] Chisato Kurosaki,[6] and Hiroshi Hirota[6]**

[1]Chemical Resources Laboratory, Tokyo Institute of Technology, 4259 Nagatsuta, Midori-ku, Yokohama 226-8503

[2]Institute for Solid State Physics, The University of Tokyo, 5-1-5 Kashiwanoha, Kashiwa 277-8581

[3]Japan Advanced Institute of Science and Technology, 1-1 Asahidai, Nomi 923-1292

[4]Department of Applied Physics, Graduate School of Engineering, Nagoya University, Furo-cho, Chikusa-ku, Nagoya 464-8603

[5]National Institute of Advanced Industrial Science and Technology (AIST), Central 5, 1-1-1 Higashi, Tsukuba 305-8565

[6]RIKEN Genomic Sciences Center, Tsurumi-ku, Yokohama 230-0045

Received December 24, 2008; E-mail: tyamamot@res.titech.ac.jp

Self-assembly of polythiophenes with –C≡CR (R = alkyl, phenyl, etc.) side chains has been investigated. Seven new polymers consisting of head-to-head and tail-to-tail 2,2′-bithiophenes with –C≡CR side chains were synthesized. The new polymers include alternating copolymers between bithiophenes with –C≡C–alkyl side chains and thiophene and those between bithiophenes with –C≡C–alkyl side chains and 2,2′-bithiophene. The polythiophene main chain is considered to be coplanar because of the absence of steric repulsion between the main chain and the –C≡CR side chain. Single-crystal X-ray crystallography and DFT calculations indicated that the head-to-head- and tail-to-tail-2,2′-bithiophenes with –C≡CR side chains were coplanar. The polythiophenes with –C≡CR side chains showed a strong tendency to self-assemble, and assumed edge-on alignment and side-on alignment on the surface of substrates. Self-assembly caused a decrease in the $\pi$–$\pi^*$ transition energy of the polymers by 0.3–0.4 eV. A copolymer of thiophene and dialkoxy-*p*-phenylene showed analogous self-assembly. The polythiophenes with –C≡CR side chains showed piezochromism, with a decrease in the $\pi$–$\pi^*$ transition energy by about 0.2 eV at 10 GPa. Head-to-head-P3(C≡C–Dec)Th with a –C≡C–decyl side chain gave a larger optical third-order nonlinear susceptibility $\chi^{(3)}$ than regio-regular poly(3-hexylthiophene)s.

Electronic and optical functionalities of $\pi$-conjugated polymers and molecules with large $\pi$-electron systems are attracting interest.[1–3] It is recognized that the electronic and optical functionalities of $\pi$-conjugated polymers and molecules are affected by molecular assembly of the polymer and molecule. The synthesis (particularly organometallic synthesis[4,5a]) of regio-regular head-to-tail poly(3-alkylthiophene-2,5-diyl), HT-P3RTh (Chart 1), by McCullough and other research groups[4,5] initiated active studies of the molecular assembly of $\pi$-conjugated polymers and its effects on the functionalities of the polymers.[1–7] HT-P3RTh shows a higher mobility[6] of positive carrier, a larger third-order nonlinear optical susceptibility, $\chi^{(3)}$,[7f] and a larger Faraday rotation[7g] than those of regio-random poly(3-alkylthiophene-2,5-diyl), rand-P3RTh, and these results have been associated with molecular assembly of HT-P3RTh in the solid phase. Recently it has been reported that various $\pi$-conjugated polythiophenes, such as those with Th(R)–($\pi$)–Th(R) repeating units, also assume similar $\pi$-stacked molecular assemblies (Chart 2).[8–11] McCulloch and co-workers synthesized such polythiophenes with fused thiophene units as the central –($\pi$)– unit,[9] and the resulting polymer showed a large hole mobility of about 1 $cm^2 V^{-1} s^{-1}$, which is comparable to that of amorphous silicon. Although HT-P3RTh provides basic and important information about the molecular assembly of $\pi$-conjugated polymers, some factors remain unclear.

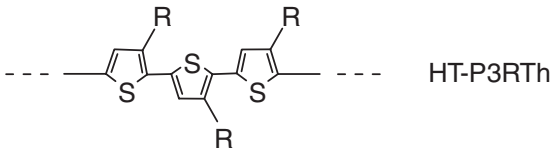


**Chart 1.**

The UV–vis absorption peak of HT-P3RTh shifts to a longer wavelength when $\pi$-stacked molecular assemblies are formed in the solid. The shift is thought to originate from the following two factors: (i) electronic interaction between face-to-face $\pi$-stacked HT-P3RTh molecules in the solid, and (ii) higher

Published on the web July 10, 2009; doi:10.1246/bcsj.82.896

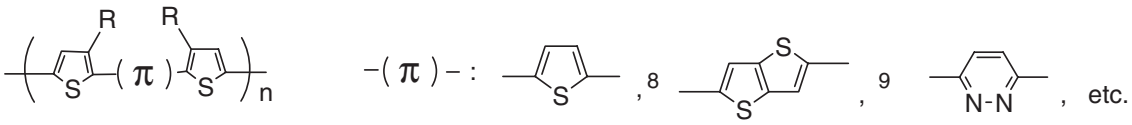

**Chart 2.**

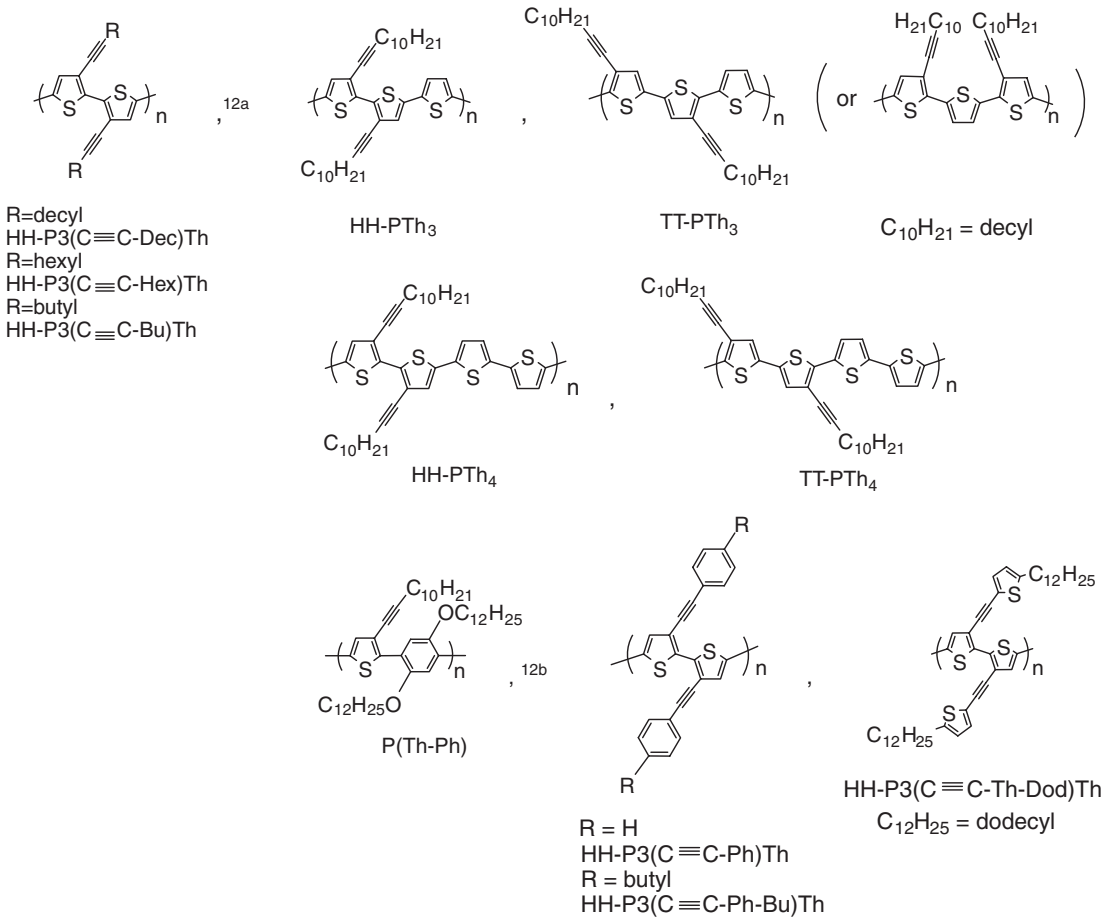


**Chart 3.** Polythiophenes used in this study.

coplanarity of HT-P3RTh in the stacked solid state.

Because HT-P3RTh seems to have some steric repulsion between the R side chain and the neighboring thiophene unit, a single HT-P3RTh molecule in solution is believed to have a somewhat twisted structure and the second factor becomes an issue.

To obtain more basic information about the molecular assembly of substituted $\pi$-conjugated polythiophenes, we have prepared the following polythiophenes with –C≡CR side chains. Synthesis of HH-P3(C≡C–alkyl)Th[12a] and P(Th–Ph)[12b] has been reported previously; HH-P3(C≡C–Dec)Th and P(Th–Ph) have number average molecular weights ($M_n$) of 7900 and 11000, respectively. Such $\pi$-conjugated polymers with –C≡CR side chains have become the subject of recent interest.[12–14]

HH-P3(C≡C–alkyl)Th, HH-PTh$_3$, TT-PTh$_3$, HH-PTh$_4$, TT-PTh$_4$, HH-P3(C≡C–Ph)Th, HH-P3(C≡C–Ph–Bu)Th, and HH-P3(C≡C–Th–Dod)Th (Chart 3) are considered to have a coplanar main chain because no steric repulsion occurs between the –C≡CR side chain and the neighboring thiophene unit in the polymers, as judged from CPK molecular models. In addition, the regio-regularity of the polymers is controlled to a great extent by the synthetic route to the polymer. For example, the head-to-head regio-regularity is believed to be 100% in HH-P3(C≡CR)Th.

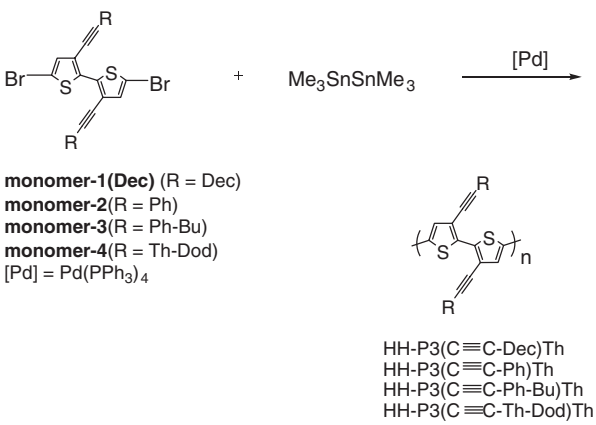


(1)

Single-crystal X-ray data for monomer-**1**(Dec), monomer-**2**,

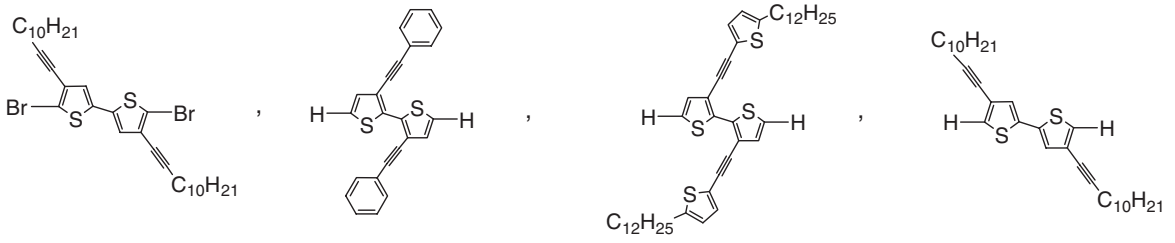


**monomer-5** (TT type isomer of **monomer-1**) | H-replaced **monomer-2** | H-replaced **monomer-4** | H-replaced **monomer-5**

**Chart 4.**

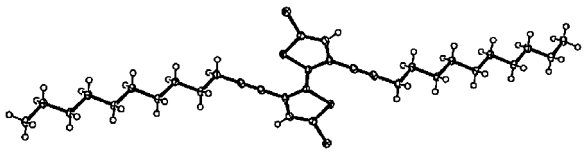

**Chart 5.** Molecular structure (top view) of monomer-**1**(Dec) (CCDC 691879). For more detail, see Figure S1.

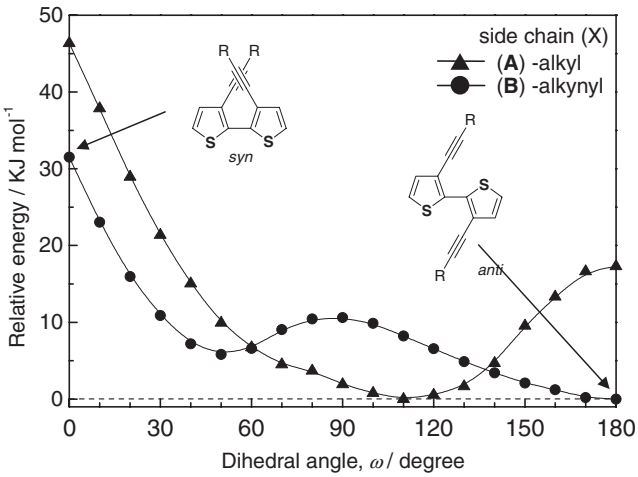


**Figure 1.** Profiles of the relative energy vs. dihedral angle ($\omega$/°) between two thiophene rings for (**A**) 3,3′-dibutyl-2,2′-bithiophene (alkyl analogue of unit A), and (**B**) 3,3′-di(1-butynyl)-2,2′-bithiophene (unit A) in the ground-state calculated at the B3LYP/6-31G* level. Side chain = $C_4$ side chain (butyl or butynyl).

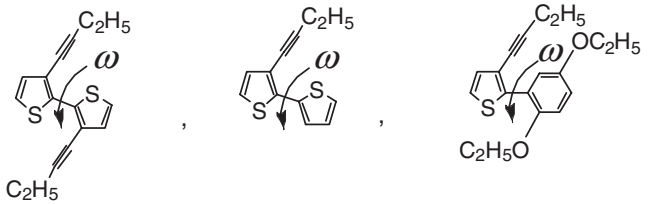


unit A | unit B | unit C

**Chart 6.**

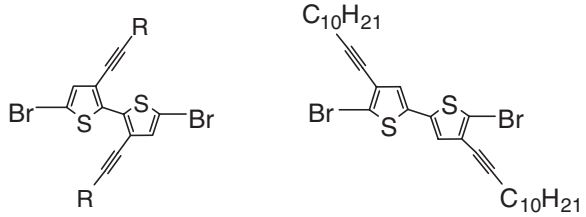


**monomer-1** through **monomer-4** | **monomer-5**

**Chart 7.**

and monomer-**4** shown in eq 1, as well as those for the related compounds (Chart 4), reveal that the 2,2′-bithiophene unit in all seven compounds has a coplanar $\pi$-conjugated structure; the single-crystal X-ray data are shown in Figures S1–S7, S10, and S11 in the Supporting Information. The molecular structure of monomer-**1**(Dec) is shown in Chart 5.

Potential energy vs. dihedral angle ($\omega$) profiles for the following unit A and unit B, which were obtained by DFT calculations and are shown in Figures 1 (for unit A) and S12 (for unit B), also indicate that the units form coplanar $\pi$-conjugated structures (Chart 6). In contrast, an alkyl analogue of unit A is believed to assume a twisted structure as shown in Figure 1. The unit C corresponding to the repeating unit in P(Th–Ph) seems to have a somewhat twisted structure as judged from DFT results shown in Figure S13. However, its stabilization energy achieved by twisting (ca. 5 kJ mol$^{-1}$; cf. Figure S13) is smaller than that (ca. 20 kJ mol$^{-1}$; cf. Figure 1) of the alkyl analogue of unit A.

We have investigated optical and basic assembling properties of the new $\pi$-conjugated polythiophenes, and herein report the results.

## Experimental

**Materials.** The polythiophenes were prepared from the monomers shown in Chart 7 via Pd-catalyzed organometallic polycondensation. Monomer-**1**s (R = Dec, Hex, and Bu),[12a] polymers HH-P3(C≡C–alkyl)Ths (alkyl = Dec, Hex, and Bu),[12a] and P(Th–Ph)[12b] were prepared as previously reported. Synthetic details for monomer-**2** through monomer-**5** and other polymers are described in Supporting Information. 2,5-Bis(trimethylstannyl)-thiophene (monomer-**6**) and 5,5′-bis(trimethylstannyl)-2,2′-bithiophene (monomer-**7**) were used as purchased.

**Measurements.** UV–vis and photoluminescence spectra,[7e,15] X-ray diffraction (XRD) patterns,[7e,15] 400 or 300 MHz NMR spectra,[15] CV (cyclic voltammetry) charts,[15] piezochromism,[15]

density of polymers,[7e,7h] and third-order optical nonlinear susceptibility ($\chi^{(3)}$)[7f] were measured in manners similar to those previously reported. Temperature-variable UV–vis spectra were measured using a multichannel fiber optics spectrometer equipped with an Ocean Optics HR2000 detector. 800 MHz $^1$H NMR spectra were recorded on a JEOL JNM-ECA800. High-temperature GPC (gel permeation chromatography) at 140 °C was carried out at TOSOH Analysis and Research Center Co. using 1,2,4-trichlorobenzene as the eluent and polystyrene standards. ESCA analysis was carried out at TOSOH Analysis and Research Center Co. using a Perkin-Elmer ESCA5400MC analyzer. Spin-coated films of HH-P3(C≡C–Dec)Th were prepared using a mixed solvent of chloroform and 1,2-dichlorobenzene (7:3 vol/vol). Spin-coating of a solution heated to its boiling point was carried out at 2000 rpm. UV–vis diffuse reflectance spectra[16] of powdery polymer samples were measured on a Shimadzu UV-3100PC spectrometer equipped with an integrating sphere assembly and transformed to UV–vis absorption spectra using Kubelka–Munk theory;[16b] $BaSO_4$ was the reference standard. Crystallographic data have been deposited with Cambridge Crystallographic Data Centre. Copies of the data can be obtained free of charge via http://www.ccdc.cam.ac.uk/conts/retrieving.html (or from the Cambridge Crystallographic Data Centre, 12, Union Road, Cambridge, CB2 1EZ, UK; Fax: +44 1223 336033; e-mail: deposit@ccdc.cam.ac.uk).

## Results and Discussion

**Preparation of Polymers.** The polymers were prepared by the following Pd-catalyzed organometallic polycondensations utilizing a Stille type reaction.[17]

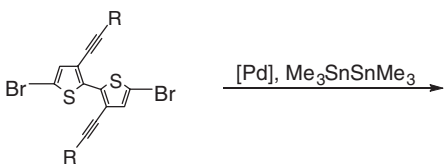


**monomer-1** through **monomer-4**

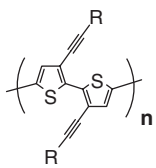


(2)

R = alkyl: HH-P3(C≡C-alkyl)Th
R = Ph: HH-P3(C≡C-Ph)Th
R = Ph-Bu: HH-P3(C≡C-Ph-Bu)Th
R = Th-Dod: HH-P3(C≡C-Th-Dod)Th

**monomer-1(Dec)** + 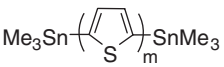


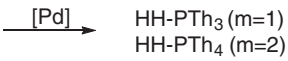


(3)

**monomer-5** + 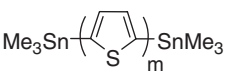


m = 1 : **monomer-6**
m = 2 : **monomer-7**


(4)

As reported previously,[12a] HH-P3(C≡C–Dec)Th was soluble in halogenated solvents such as 1,2-dichlorobenzene at 140 °C and was susceptible to GPC analysis. However, HH-$PTh_3$, TT-$PTh_3$, HH-$PTh_4$, and TT-$PTh_4$ were insoluble in organic solvents even at 140 °C, presumably because of their well-packed solid structures. Their ESCA, IR, and solid-state $^{13}$C NMR data agreed with their molecular structures. Because the content of Br was about 0.1 mol % or below the limit of detection, they were presumed to have long polymer chains; their diffuse reflectance spectra (vide infra) also indicated that they had long $\pi$-conjugated polymer chains.

HH-P3(C≡C–Ph)Th and HH-P3(C≡C–Ph–Bu)Th gave brown-colored solutions of halogenated hydrocarbons such as 1,2-dichlorobenzene when heated at 140 °C. However, they were not suited for GPC analysis at 140 °C using 1,2,4-trichlorobenzene as the eluent, presumably due to partial aggregation even at a high temperature. Their IR, solid-state $^{13}$C NMR, and ESCA data were consistent with their structures; their contents of Br were also very low (about 0.1 mol %) or below the limit of detection. HH-P3(C≡C–Th–Dod)Th was soluble in 1,2-dichlorobenzene and 1,2,4-trichlorobenzene at 140 °C, and was characterized by IR, $^1$H NMR, $^{13}$C NMR, and GPC. GPC data showed $M_n$ of 6000 and $M_w$ (weight average molecular weight) of 17000.

All polymers having the polythiophene main chain showed similar dark brown color in solid, similar to the brown color of nonsubstituted polythiophene, PTh, and HT-P3RTh. Monomer-**1** through monomer-**5** were colored yellow or orange. UV–vis diffuse reflectance spectra of all the polymers with the –C≡CR side chains, measured with powdery samples, showed UV–vis absorption peaks near that of HT-P3RTh as described in the following.

CP/MAS solid-state $^{13}$C NMR spectrum of HH-P3(C≡C–alkyl)Th showed sharp thiophene (Th)-carbon and acetylenic-carbon signals. The sharpness of the Th-carbon signals is comparable to that of HT-P3RTh and sharper than that of rand-P3RTh. Figure 2 shows a comparison of the CP/MAS solid-state $^{13}$C NMR spectrum of HH-P3(C≡C–Dec)Th with those of rand-P3HexTh[7e] (Hex = hexyl; HT content = ca. 30%) and

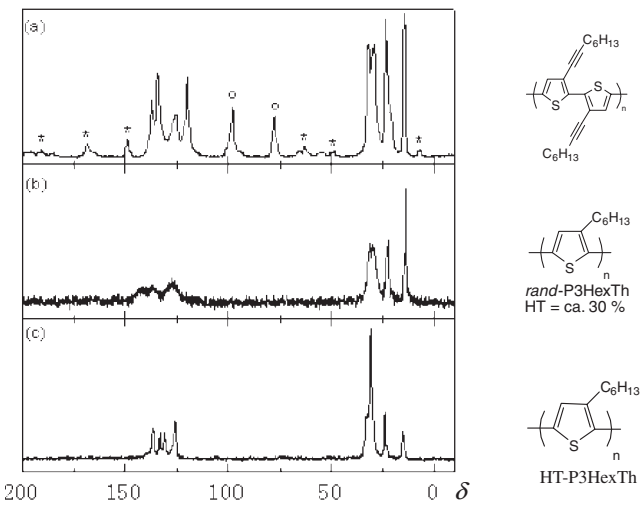


**Figure 2.** CP/MAS solid-state $^{13}$C NMR spectra of (a) HH-P3(C≡C–Hex)Th, (b) regio-random P3HexTh (HT content = ca. 30%),[7e] and (c) HT-P3HexTh. Th-carbon signals appear in a range from about $\delta$ 120 to 140. The peaks marked with a circle in Figure 2a are assigned to –C≡C– carbons. Peaks marked with * are due to spinning side bands of the Th- and –C≡C– carbon signals.

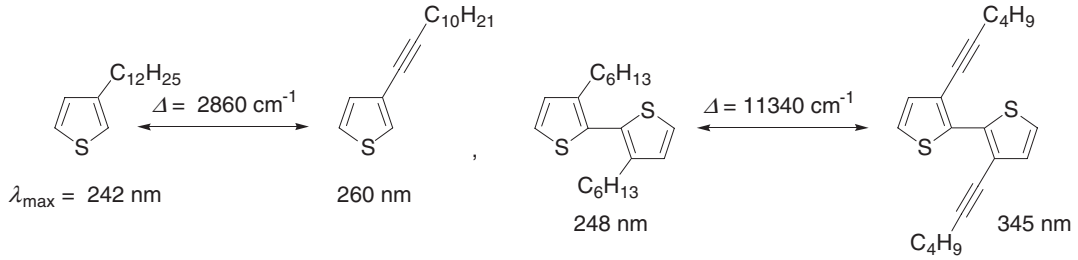


**Chart 8.** Comparison of the UV–vis absorption peaks of 3-alkylthiophenes and 3-alkynylthiophenes.

HT-P3HexTh.

As shown in Figure 2a, HH-P3(C≡C–Hex)Th gives rise to two sharp –C≡C– carbon signals at $\delta$ 77.3 and 99.7.[18] CP/MAS solid-state $^{13}$C NMR spectra of HH-PTh$_3$, TT-PTh$_3$, HH-PTh$_4$, TT-PTh$_4$, HH-P3(C≡C–Ph)Th, and HH-P3(C≡C–Ph–Bu)Th also show sharp Th- and –C≡C– carbon signals, as shown in Figure S14. The two –C≡C– carbon signals are separated by about 20 ppm for HH-P3(C≡C–alkyl)Ths, HH-PTh$_3$, TT-PTh$_3$, HH-PTh$_4$, and TT-PTh$_4$, whereas they are separated by about 10 ppm for HH-P3(C≡C–Ph)Th and HH-P3(C≡C–Ph–Bu)Th because of the attachment of an aromatic ring at both the –C≡C– carbons. In the case of HH-P3(C≡C–Th–Dod)Th, the two –C≡C– carbon signals seem to overlap each other as shown in the synthetic part of HH-P3(C≡C–Th–Dod)Th in Supporting Information.

**UV–Vis Spectra and $^1$H NMR.** The UV–vis absorption peak of 3-alkylthiophene is shifted to a wavelength longer by 18 nm or 2860 cm$^{-1}$ when the alkyl group is replaced by the –C≡C–alkyl group, presumably because of certain expansion of the $\pi$-conjugation system.

As shown on the right of Chart 8, the HH-dimers of 3-alkylthiophene and 3-alkynylthiophene show a larger $\pi$–$\pi^*$ transition energy difference of 11340 cm$^{-1}$, which is ascribed to a twisted structure of the 3-alkylthiophene dimer and coplanar structure of the 3-alkynylthiophene dimer.

When the dimer is formed, $\lambda_{max}$ of 3-alkynylthiophene shifts from 260 to 345 nm (cf. Chart 8) with a $\pi$–$\pi^*$ transition energy shift of $\Delta E = 9480\,\mathrm{cm}^{-1}$. This $\Delta E$ is comparable to that observed between nonsubstituted thiophene ($\lambda_{max} = 231$ nm) and 2,2′-bithiophene ($\lambda_{max} = 302$ nm[2a] and $\Delta E = 10180\,\mathrm{cm}^{-1}$) and gives additional support for the coplanar structure of the dimer of 3-alkynylthiophene.

HH-P3(C≡C–Dec)Th,[12a] HH-P3(C≡C–Th–Dod)Th, and HH-P3(C≡C–Ph)Th were not soluble in organic solvents at room temperature. However, they were soluble in 1,2-dichlorobenzene at high temperature (e.g., 130 °C), and the soluble state had some stability even when their solutions were cooled to room temperature; temperature dependent UV–vis spectra of HH-P3(C≡C–Dec)Th,[17e,17f] have been reported. Figure S15 shows temperature dependent UV–vis spectra of HH-P3(C≡C–Dec)Th, HH-P3(C≡C–Th–Dod)Th, and HH-P3(C≡C–Ph)Th in 1,2-dichlorobenzene. At high temperature of about 130 °C, they showed a UV–vis peak at about 500–520 nm, and the UV–vis peak shifts to a longer wavelength upon cooling. HH-P3(C≡C–Dec)Th and HH-P3(C≡C–Th–Dod)Th gave rise to new shoulder peaks at 600 and 650 nm, respectively.

$CHCl_3$ and $CH_2Cl_2$ solutions of HT-P3HexTh showed similar temperature-dependent changes in their UV–vis spectra when cooled to below about 0 °C,[1,7e] and it was assigned to self-assembly of HT-P3HexTh at temperatures below about 0 °C. Similar self-assembly of HH-P3(C≡C–Dec)Th and HH-P3(C≡C–Th–Dod)Th at temperatures below 60 and 35 °C, respectively, is conceivable, and the occurrence of spectral changes at considerably higher temperatures than those of the $CHCl_3$ and $CH_2Cl_2$ solutions of HT-P3HexTh indicates that HH-P3(C≡CR)Th has a stronger tendency to self-assemble than HT-P3HexTh. The UV–vis spectra of the 1,2-dichlorobenzene solutions of HH-P3(C≡C–Dec)Th and HH-P3(C≡C–Th–Dod)Th at 25 °C showed no time-dependence after cooling to 25 °C from about 130 °C, indicating that the self-assembly took place rapidly upon cooling the solution.

Temperature-dependent $^1$H NMR spectra of HH-P3(C≡C–Dec)Th also showed signs of self-assembly at lower temperatures. As shown in Figure S16a, HH-P3(C≡C–Dec)Th shows a $^1$H NMR spectrum, with reasonable peak area ratios, at 130 °C. However, the aromatic Th–H ($\delta$ 7.1) and –C≡C–$CH_2$– ($\delta$ 2.5) signals are weakened, compared with the terminal $CH_3$ signal, at 110 °C and below the temperature in $CDCl_2CDCl_2$.

Similar weakening of Th–H and Th–$CH_2$– peaks of HT-P3HexTh at −20 °C in $CDCl_3$ has been reported (cf. Figure S16b),[7e] and it was considered to originate from loss of motional freedom of the Th–H and Th–$CH_2$– protons in stacked colloidal particles of HT-P3HexTh at −20 °C. Similar loss of motional freedom of the Th–H and –C≡C–$CH_2$– protons of HH-P3(C≡C–Dec)Th in the stacked colloidal particles formed at lower temperatures accounts for the NMR data.

UV–vis peaks of spin-coated and cast films of HH-P3(C≡C–Dec)Th[17f] and HH-P3(C≡C–Th–Dod)Th on a quartz glass plate (cf. Figures S17 and S18) are shifted, e.g., by about 80 nm, to a longer wavelength from that of the 1,2-dichlorobenzene solution. Cast film showed a larger red shift than spin-coated film. After annealed at 130 °C, the UV–vis spectrum of the spin-coated film essentially agreed with that of the cast film. By annealing, the XRD peak becomes sharper as shown in Figure S17. Similar differences in optical and XRD data between spin-coated film, its annealed film, and cast film of $\pi$-conjugated polymers have been reported.[19]

As shown in Figure S17, both the spin-coated and cast films of HH-P3(C≡C–Dec)Th show sub-structures with an energy difference of about 1370 cm$^{-1}$. The energy difference essentially agrees with the Raman spectrum of HH-P3(C≡C–Dec)Th, which contains a peak at 1388 cm$^{-1}$, as depicted in Figure S19. The Raman peak is assignable to an asymmetric C=C vibration,[20] and the higher frequency of the Raman peak of HH-P3(C≡C–Dec)Th than that (1379 cm$^{-1}$; cf. Figure S19) of HT-P3HexTh suggests a higher order of $\pi$-conjugation in HH-

P3(C≡C–Dec)Th than in HT-P3HexTh. After the spin-coated film was annealed, the Raman peak became sharper as shown in Figure S19.

Because of the insolubility of HH-PTh$_3$, TT-PTh$_3$, HH-PTh$_4$, and TT-PTh$_4$, their optical data in solution were not obtained. However, comparison of their UV–vis diffuse reflectance spectra[16] with that of HH-P3(C≡C–Dec)Th ($\lambda_{max}$ = ca. 650 nm) in a powdery state indicates that the UV–vis absorption peak of the polymers shifts to a longer wavelength in the order shown in Chart 9 (cf. Figure S20). These data are considered to reflect the number density of the alkynyl group along the $\pi$-conjugated main chain. The $\lambda_{max}$ in the diffused reflectance spectra of PTh$_4$'s is comparable to or somewhat longer than that of HT-P3HexTh shown in Figure S20h. Polythiophenes with a $\pi$-conjugated system in the side chain sometimes give rise to a UV–vis peak at a longer wavelength than that of usual polythiophenes without such a $\pi$-conjugated system.[21b]

A fraction of HH-P3(C≡C–Dec)Th soluble in chloroform at room temperature and having a lower $M_n$ of 4400 showed a photoluminescence peak at $\lambda_{EM}$ = 583 nm with a quantum yield of 14% in chloroform. The excitation spectrum showed a peak at $\lambda_{EX}$ = 518 nm, which agrees with the UV–vis data of HH-P3(C≡C–Dec)Th. A cast film of the chloroform soluble part also showed a shift to a longer wavelength, as shown in Figure 3. However, the degree of the shift was smaller than that observed with the original HH-P3(C≡C–Dec)Th with $M_n$ of 7900, revealing that the self-assembling force between the polymer molecules becomes stronger with increasing molecular weight.

PTh$_4$'s (ca. 610 nm) < PTh$_3$'s (ca. 635 nm)
< HH-P3(C≡C-Dec)Th (ca. 650 nm)

**Chart 9.** $\lambda_{max}$/nm (data of diffuse reflectance spectra[16]).[21a]

**XRD Data and Alignment on Substrate. HH-P3(C≡C–alkyl)Th:** Figure 4 shows XRD patterns of HH-P3(C≡C–Dec)Th[17f] and HH-P3(C≡C–Hex)Th measured for powdery samples (top curves), cast films (middle curves), and pressed (or rubbed) powders (bottom curves). Comparison of the XRD patterns shown in Figure 4 with those of HT-P3HexTh and HH-P3(C≡C–Bu)Th is shown in Figure S21.

As shown in Figure 4, the powder XRD pattern of HH-P3(C≡C–alkyl)Th shows a diffraction peak in the low angle region with spacing $d_1$. Such an XRD peak in a low angle region is often observed in XRD patterns of $\pi$-conjugated polymers with long side chains (e.g, HT-P3HexTh),[1,2,7] and the peak has been assigned to a distance between $\pi$-conjugated main chains separated by the long side chains. For HH-

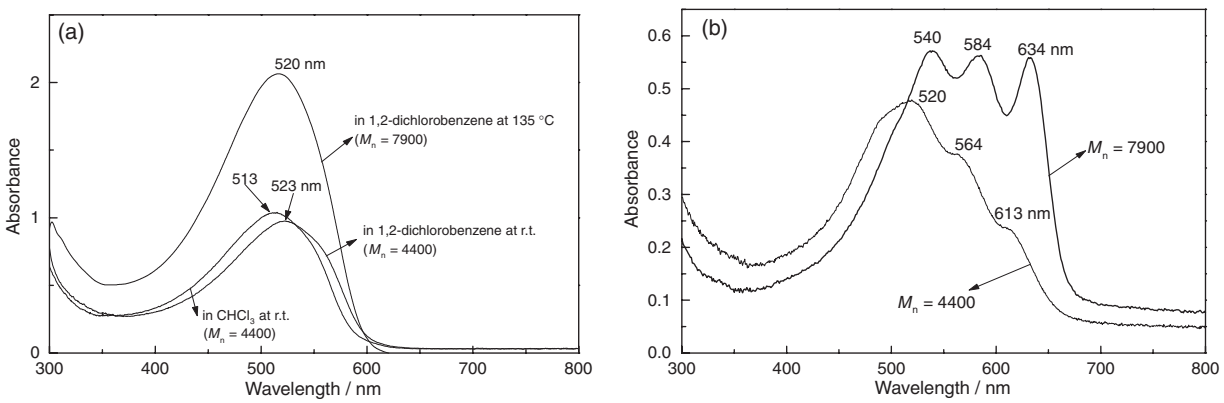


**Figure 3.** Comparison of UV–vis spectra of original HH-P3(C≡C–Dec)Th with $M_n$ of 7900 and a chloroform soluble fraction of HH-P3(C≡C–Dec)Th with $M_n$ of 4400. (a): Solution. (b): Cast film.

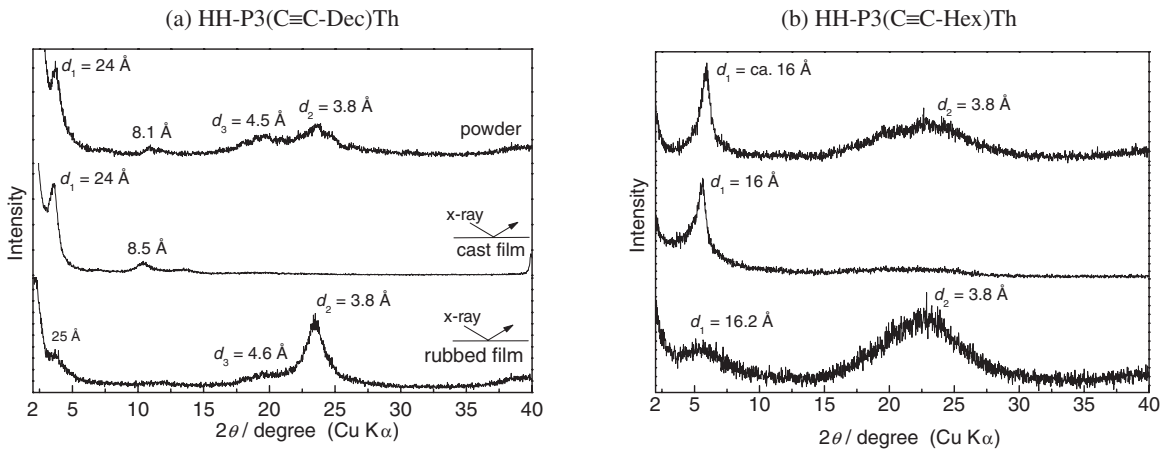


**Figure 4.** XRD patterns of HH-P3(C≡C–Dec)Th (left) and HH-P3(C≡C–Hex)Th (right) under various conditions. Top: powder sample. Middle: cast film on a Pt plate. Bottom: rubbed powdery sample (rubbed with a spatula) on an amorphous-Si plate.

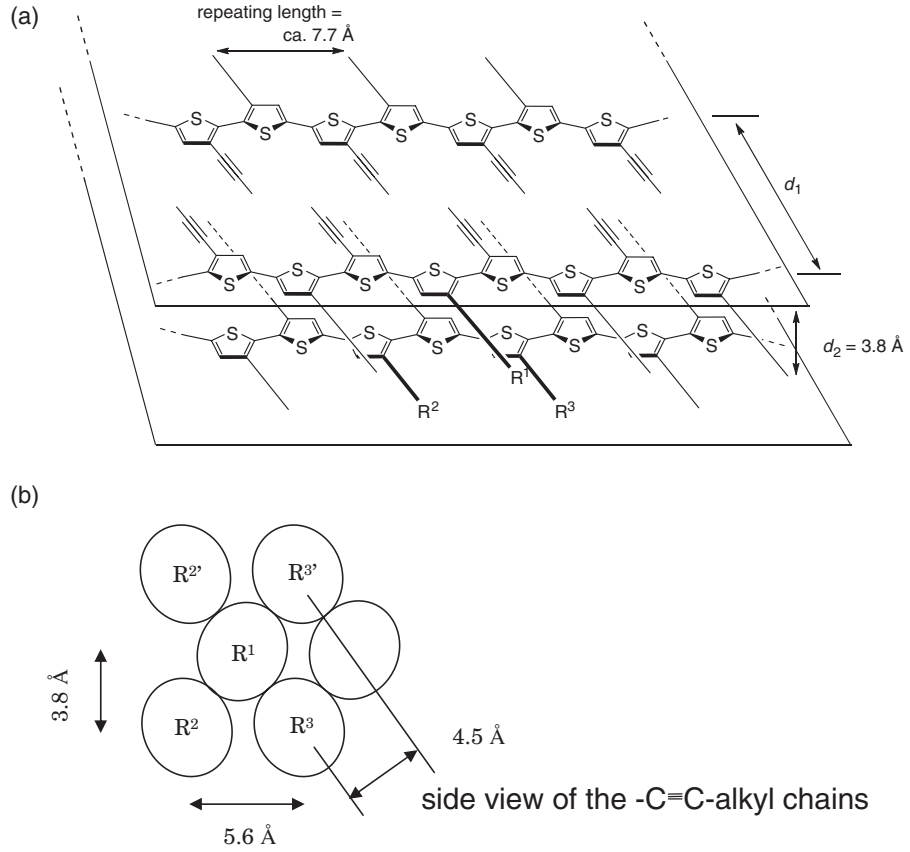


**Figure 5.** (a) Packing model of HH-P3(C≡C–alkyl)Th in solid state and (b) side view of the packed –C≡C–alkyl side chains, seen from the direction of the –C≡C–alkyl side chain. Only two layers in the stacked polymer solid are shown. The thiophene unit in the lower layer is believed to locate below the thiophene unit in the upper layer, with the opposite direction of S. In this situation, the alkyl groups in the side chains are presumed to be packed in a mode as shown in part (b). The repeating length was estimated from single-crystal X-ray data of thiophene oligomers,[2a,22a,22b] and aggregation of the alkyl group[22c,22d] is assumed.

P3(C≡C–alkyl)Th, its XRD data are explained by the packing model shown in Figure 5.

The number density of the –C≡C–alkyl side chain is the same as that of HT-P3RThs, which form an end-to-end packing structure similar to that shown in Figure 5. The increase in $d_1$ with the increase in the length of the alkyl group in the –C≡C–alkyl side chain, $\Delta(d_1)/\Delta$(number of carbon atoms in the alkyl group) = about 2.0 Å/C, is larger than the repeating length of the $–CH_2–$ group in alkyl chains (1.25 Å/C). These data exclude an interdigitation packing model and support the end-to-end packing model shown in Figure 5.

A $\pi$-stacking[22e–22i] force between the HH-P3(C≡C–alkyl)Th molecules may also contribute to the stabilization of the packed structure. The $\pi$-stacking distance, $d_2 = 3.8$ Å, estimated from the XRD pattern is similar to that reported for HT-P3RThs.[1,2,7] The XRD peak at 8.1 Å (cf. the left part of Figure 4) of HH-P3(C≡C–Dec)Th is assigned to a $d_1/3$ peak.

The stacking of the main chain affords the 7.7 Å (repeating length) × 3.8 Å ($d_2$) = 29 Å$^2$ cross section for the side chain at most. Since the effective cross section of alkyl chains is about 20 Å$^2$ as will be mentioned later, the area of 29 Å$^2$ is insufficient for interdigitation packing, while it is too much for the end-to-end packing. Because of the main-chain chemical geometry and also in order to achieve side-chain close aggregation, the side chain will be tilted by an angle $\alpha$ of ca. 40° from the normal to the main-chain axis. This is roughly consistent with the $\Delta(d_1)$ per number of carbon atoms in the alkyl group, which is expected to be 2.55 Å (2 × repeating height of $CH_2$) × $\cos\alpha$ = 1.95 Å/C. As a result, the side-by-side distance between the neighboring side chains $R^2$ and $R^3$ is estimated to be 7.7 × $\cos\alpha$ = 5.5–6 Å, as is shown in Figure 5b. The mean $R^2$–$R^3$ distance 5.6 Å offers the reasonable cross section of 5.6 Å × 3.8 Å = 21 Å$^2$ for a side chain, and also explains the XRD peak at about $d_3 = 4.5$ Å in a manner similar to the strong 110 reflection of the orthorhombic polyethylene crystal.

The observed density of HH-P3(C≡C–Dec)Th, $\rho_{obs} = 1.14$ g cm$^{-3}$, basically agreed with the density, $\rho_{calcd} = 1.17$ g cm$^{-3}$, calculated[23] according to the packing model shown in Figure 5. HH-P3(C≡C–Hex)Th reasonably gives shorter $d_1$ as shown in the right side of Figure 4. Because of the shortening of $d_1$, the density of HH-P3(C≡C–Hex)Th, $\rho_{obs} = 1.34$ g cm$^{-3}$, increased, and it also agreed with the calculated density, $\rho_{calcd}$ = 1.35 g cm$^{-3}$.

The $d_1$ values of HH-P3(C≡C–Dec)Th and HH-P3(C≡C–Hex)Th are somewhat shorter than those of HT-P3DodTh ($d_1 = 27$ Å) and HT-P3OctTh ($d_1 = 20$ Å) (Dod = dodecyl; Oct = octyl).[2,7e] These results may arise from a somewhat smaller tilting angle of the –C≡C–alkyl group from the polythiophene main chain than that of the alkyl group.

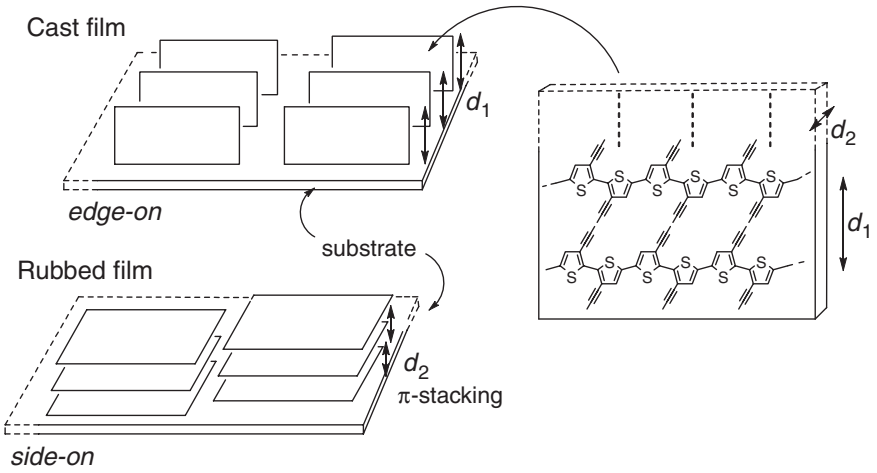


**Figure 6.** Two types of alignment[17g] of HH-P3(C≡CR)Th on the surface of substrates.

In the case of HH-P3(C≡C–Bu)Th, the $d_1$ peak at about 13 Å is broadened (cf. Figure S21), suggesting that the shorter side chain is not suited for forming a well-packed structure. However, the observed density ($\rho_{obs} = 1.52\,g\,cm^{-3}$) roughly agreed with the calculated density ($\rho_{calcd}$ = ca. $1.5\,g\,cm^{-3}$).

An interesting phenomenon suggested by the XRD data of HH-P3(C≡C–alkyl)Th is molecular ordering of the polymer on the surface of substrates. As shown by the middle XRD curves in Figure 4, the $d_2$ peak essentially disappeared for the cast film of HH-P3(C≡C–alkyl)Th. On the other hand, the $d_1$ peak is clearly observed. Cast films of various π-conjugated polymers with long side chains give similar XRD results,[1–7,9] and it is taken as an indication of alignment of the π-conjugated polymer on the surface of substrates, with the side chains oriented toward the surface of the substrate. For the cast film of HH-P3(C≡C–alkyl)Th, similar alignment of the HH-P3(C≡C–Dec)Th molecules is believed to take place, as shown in Figure 6.[17f,17g]

Rubbing the cast film or powdery sample of HH-P3(C≡C–alkyl)Th with a spatula[24] caused another type of alignment as revealed by the bottom curve of Figure 4. In the new XRD curve, the $d_2$ peak is strengthened and the $d_1$ peak is weakened. These results suggest another type of alignment of the HH-P3(C≡C–alkyl)Th molecule, which is depicted in the lower part of Figure 6. Such side-on type alignment is considered to indicate that the HH-P3(C≡C–alkyl)Th molecules form a well-packed layered structure, similar to those of graphite and mica. High coplanarity of the HH-P3(C≡C–alkyl)Th molecule and –C≡C–alkyl group-assisted strong self-assembly of HH-P3(C≡C–alkyl)Th seem to make the layered planar structure stable. Brinkmann reported that HT-P3HexTh also formed a side-on aligned structure under certain conditions.[25] However, rubbing HT-P3HexTh under the same conditions applied to HH-P3(C≡C–alkyl)Th did not cause such alignment. The rubbed powdery sample of HT-P3HexTh gave rise to an XRD pattern essentially agreeing with that of powdery HT-P3HexTh. The side-on alignment of HH-P3(C≡C–alkyl)Th, however, seems to be less stable than edge-on alignment since the side-on type alignment is changed to the edge-on type alignment in repeated electrochemical measurements.

Because of the difference in the alignment between the cast film and rubbed film, they showed different electrochemical responses. As shown in Figure S22, CV data of HH-P3(C≡C–Dec)Th from the $CH_3CN$ solution of $[(n\text{-}Bu)_4N]BF_4$ indicated that the rubbed film underwent more facile p-doping (or oxidation) with two peak potentials at 0.63 and 0.85 V vs. $Ag^+/Ag$ in the first CV cycle. In contrast, the p-doping peak of the cast film appeared at 0.9–0.94 V vs. $Ag^+/Ag$ in the first cycle (Chart 10).

Peak oxidation (or p-doping) potential of HH-P3(C≡C-Dec)Th: *E*/V vs. $Ag^+/Ag$
Side-on (0.63 and 0.85) < Edge-on (0.94)

**Chart 10.** Effect of the mode of alignment on electrochemical oxidation of HH-P3(C≡C–Dec)Th (cf. Figure S22).

These results suggest that electron transfer from the Pt substrate and/or movement of the $BF_4^-$ dopant in the polymer solid is easier in the rubbed film. In side-on packing, the electron transfer may be easier because of the face-to-face interaction of the HH-P3(C≡C–Dec)Th molecules and the electrode.

As shown in Figure S22, the p-doping potential of the rubbed film shifted to a higher potential upon repeated scanning, suggesting that the side-on aligned mode of the rubbed HH-P3(C≡C–Dec)Th film changed to the edge-on aligned mode shown in Figure 6 during the electrochemical p-doping (side-on to edge-on transition). After p-doping, the XRD pattern of the rubbed film clearly showed a $d_1$ peak in the low angle region, and the $d_2$ peak became very weak, supporting this assumption (cf. Figure S23). As shown in Figure S23, the $d_1$ peak became longer from 24 Å to about 27 Å after p-doping, whereas the weak $d_2$ peak seemed to become shorter from 3.8 to 3.5 Å. Similar p-doping effects on $d_1$ and $d_2$ were observed with HT-P3HexTh[26] and a copolymer of isothianaphthene and dialkoxy-*p*-phenylene.[27]

These XRD data are thought to indicate that the dopant ($BF_4^-$ in this case) is located at the ends of the long side chains and expands the $d_1$ distance, and the p-doping increases the π-stacking force between the π-conjugated polymers. Location of an $RSO_3^-$ dopant near a side group was reported for p-doped

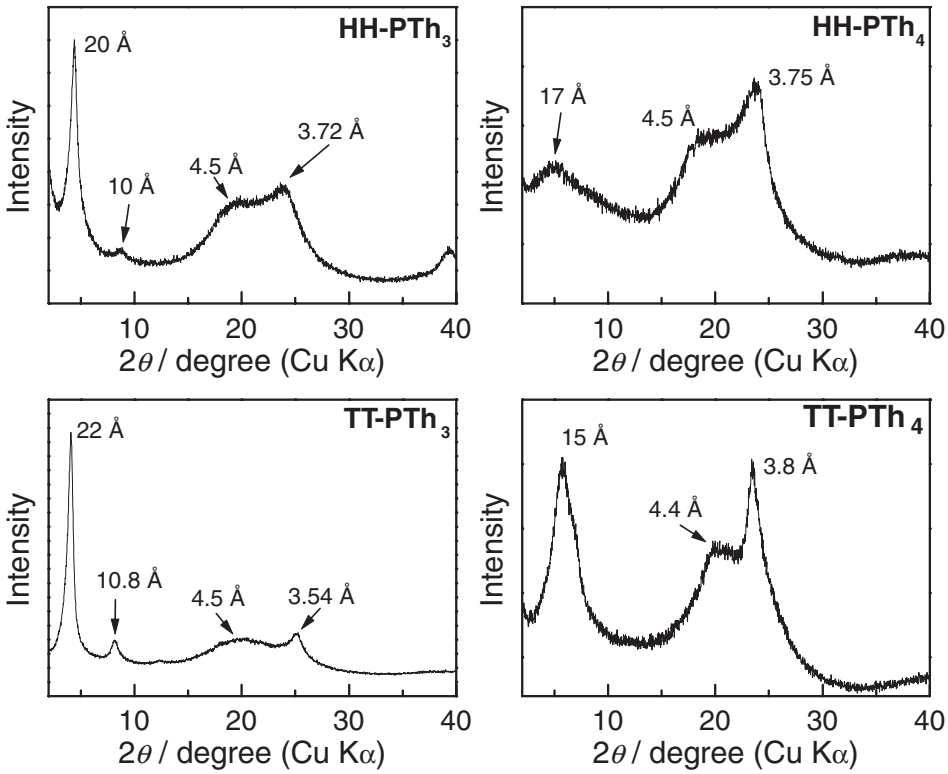


**Figure 7.** Powder XRD patterns of HH-PTh$_3$, TT-PTh$_3$, HH-PTh$_4$, and TT-PTh$_4$.

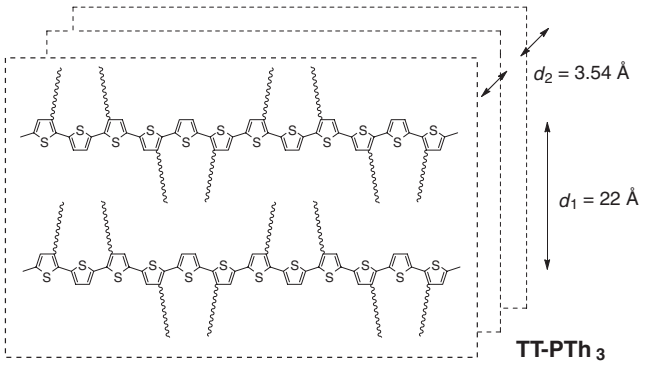


**Figure 8.** An interdigitation packing model of TT-PTh$_3$.

PEDOT, poly(3,4-ethylene-dioxythiophene).[22b] Shortening the $\pi$-stacking distance according to the p-doping of PEDOT was reported.[22b,28]

**HH-PTh$_3$, TT-PTh$_3$, HH-PTh$_4$, and TT-PTh$_4$:** Figure 7 shows powder XRD patterns of HH-PTh$_3$, TT-PTh$_3$, HH-PTh$_4$, and TT-PTh$_4$. The XRD data shown in Figure 7 reveals the following features of the polymers.

(1) The polymers also show a $d_1$ peak at the low angle region. HH-PTh$_3$ and TT-PTh$_3$ show a $d_1/2$ peak.

(2) $d_1$ values of HH- and TT-PTh$_3$ are shorter than that (24 Å) of HH-P3(C≡C–Dec)Th. This suggests that HH- and TT-PTh$_3$ assume an interdigitation packing mode in the solid state because of lower number density of the –C≡C–Dec side chain in HH- and TT-PTh$_3$. The number density of side chains often determines the end-to-end or interdigitation packing mode of five-membered ring $\pi$-conjugated polymers.[1,2,7e,29] A packing model for TT-PTh$_3$ is shown in Figure 8.

Values of $d_1$ of HH- and TT-PTh$_4$ then become shorter, presumably because of a larger space allotted for –C≡C–Dec side chains. The sharper $d_1$ peak of HH- and TT-PTh$_3$ than that of HH- and TT-PTh$_4$ suggests that HH- and TT-PTh$_3$ are more suited to form an organized packing structure.

(3) The characteristic $d_2$ peaks are also observed for HH-PTh$_3$, TT-PTh$_3$, HH-PTh$_4$, and TT-PTh$_4$ in the range of 3.5–3.8 Å. HH-PTh$_3$, TT-PTh$_3$, HH-PTh$_4$, and TT-PTh$_4$ showed densities of 1.12, 1.09, 1.12, and 1.23 g cm$^{-3}$, respectively, which agreed within experimental error with calculated densities of 1.15, 1.09, 1.12, and 1.25 g cm$^{-3}$, which were calculated on the basis of $d_1$, $d_2$, and repeating length of thiophene assumed for HH-P3(C≡C–Dec)Th. For rubbed powders of TT-PTh$_3$ and TT-PTh$_4$, the $d_2$ XRD peak was enhanced and the $d_1$ peak was weakened, similar to the case of HH-P3(C≡C–Dec)Th. However, for HH-PTh$_3$ and HH-PTh$_4$, a rubbing effect was not observed.

**HH-P3(C≡C–Ph)Th, HH-P3(C≡C–Ph–Bu)Th, HH-P3(C≡C–Th–Dod)Th, and P(Th–Ph):** HH-P3(C≡C–Ph)Th and HH-P3(C≡C–Ph–Bu)Th produce powder XRD patterns similar to that of HH-P3(C≡C–R)Th, as shown in Figure S24. The XRD patterns show a peak at the low angle region and the typical $d_2$ peak at 3.6–3.7 Å. Although the *p*-phenylene unit has a larger cross section than the *n*-alkyl group, the difference in the cross section between the *p*-phenylene unit and *n*-alkyl group is not large. For example, polyethylene and poly(*p*-phenylene) PPP have the following lateral dimensions in herringbone packing.[1–3]

As shown in Chart 11, the alkyl chain has an effective cross section of $(a \times b)/2 = 18\,\text{Å}^2$, whereas the effective cross section of the *p*-phenylene unit is estimated to be $21\,\text{Å}^2$.

Although the *p*-phenylene unit has a larger cross section than the alkyl chain, suitable rotation of the *p*-phenylene unit seems to make the formation of the $\pi$-stacked structure, which is similar to that shown in Figure 5, possible. In the case of HH-P3(C≡C–Ph)Th, rubbing the polymer sample did not cause obvious change in the XRD pattern. On the other hand, rubbing the HH-P3(C≡C–Ph–Bu)Th brought about a large change in the XRD pattern as shown in Figure S24d, which was accounted for by the side-on alignment (cf. Figure 6) of HH-P3(C≡C–Ph–Bu)Th on the surface of the substrate.

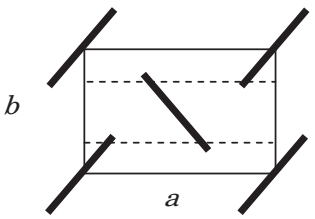


| | *a*/Å | *b*/Å |
|---|---|---|
| polyethylene | 7.4 | 4.9 |
| PPP | 7.8 | 5.5 |
| PTh | 7.8 | 5.5 |

**Chart 11.** Herringbone packing of polyethylene, poly(*p*-phenylene) PPP, and poly(thiophene) PTh.

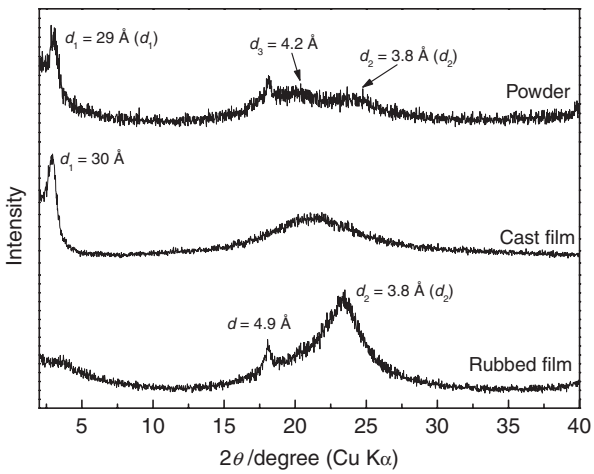


**Figure 9.** XRD data for HH-P3(C≡C–Th–Dod)Th. Top: powder sample. Middle: film cast on a Pt plate. Bottom: sample prepared by rubbing powdery HH-P3(C≡C–Th–Dod)Th with a spatula on an amorphous Si substrate.

HH-P3(C≡C–Th–Dod)Th gives analogous XRD results, and the data are shown in Figure 9.

Because of the strong diffraction originating from the long dodecyl group, the $d_2$ peak at about 3.8 Å becomes obscure for the powdery sample. However, it becomes the main peak for the rubbed polymer sample. An additional peak is observed at $d$ = 4.9 Å may come from the oblique alignments of the side chain.

If $\pi$-stacking structures similar to that shown in Figure 5 are assumed for HH-P3(C≡C–Ph)Th, HH-P3(C≡C–Ph–Bu)Th, and HH-P3(C≡C–Th–Dod)Th, the XRD data give calculated densities of 1.46, 1.55, and 1.40 g cm$^{-3}$ for the polymers, respectively, which agree with observed densities of 1.43, 1.54, and 1.39 g cm$^{-3}$, respectively.

P(Th–Ph) does not seem to have a regio-controlled structure, because its $^1$H NMR spectrum shows four –OCH$_2$– peaks at $\delta$ 4.10, 4.04, 3.94, and 3.90 at 800 MHz separated by 48, 80, and 32 Hz, as shown in Figure S25. If the direction of the –C≡C–C$_{10}$H$_{21}$ side chain attached to the thiophene unit is controlled to an HT-mode, only two –OCH$_2$– peaks appear. Even for regio-irregular P(Th–Ph), its powder XRD pattern shows typical $d_1$ and $d_2$ peaks, as shown in Figure 10, although $d_2$ is longer than that observed for the polymers having the polythiophene main chain.

For regio-irregular poly(3-alkylthiophene) P3RTh, collision of the alkyl side chains, is thought to bring about twisting of the polythiophene main chain.[1–3] However, in the case of P(Th–Ph), rotation of the dialkoxy-*p*-phenylene unit may be possible to allow the $\pi$-stacking of P(Th–Ph).

Because of the high number density of the long side chain, P(Th–Ph) is thought to pack end-to-end, and the $d_1$ of 33 Å (cf. Figure 10), which is longer than that of HH-P3(C≡C–Dec)Th (cf. Figure 4), is reasonable in view of the higher number density of the long side chains of P(Th–Ph).

$d_2$ of P(Th–Ph) is longer than those observed for the HH-P3(C≡CR)Th (R = alkyl, etc.) polymers, which may be related to the less well-packed structure of P(Th–Ph). However, the $\pi$-stacking force between the P(Th–Ph) seems to be strong, and rubbing powdery P(Th–Ph) leads to the side-on alignment of P(Th–Ph), as shown Figure 10b. When P(Th–Ph) powder was pressed, the pellet and film obtained had a metallic color, as shown in Figure S26. The UV–vis absorption peak of P(Th–

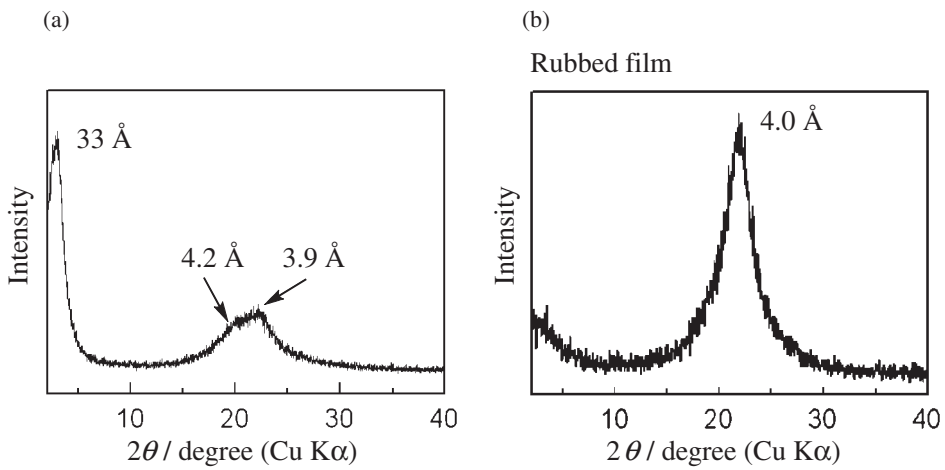


**Figure 10.** XRD patterns of (a) powdery P(Th–Ph) and (b) P(Th–Ph) obtained by rubbing powdery P(Th–Ph) with a spatula.

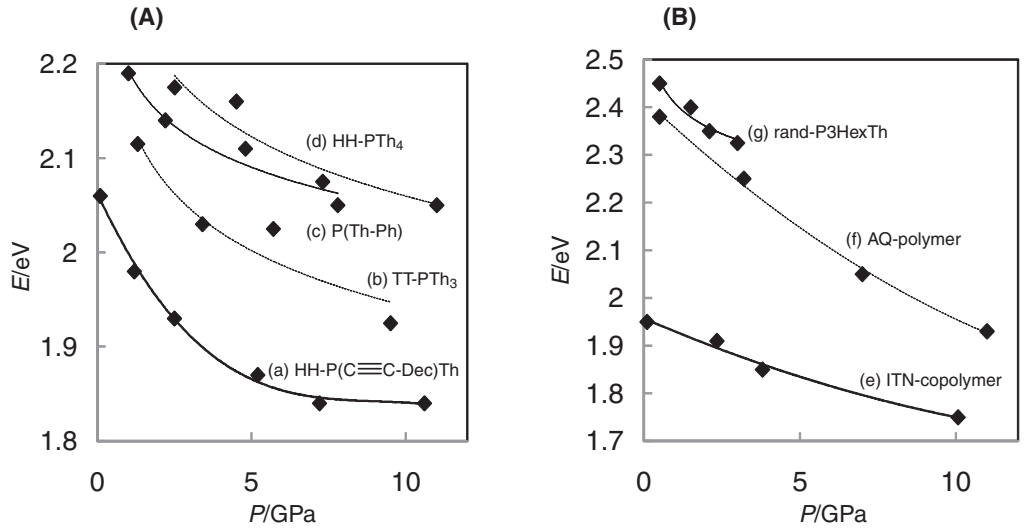


**Figure 11.** (A) Piezochromic data of polymers reported in this paper. For comparison, piezochromic data of other $\pi$-conjugated polymers are shown in (B). (a): HH-P3(C≡C–Dec)Th. (b): TT-PTh$_3$. (c): P(Th–Ph). (d): HH-PTh$_4$. (e): Isothianaphthene copolymer. (f): Anthraquinone polymer.[15] (g): Regio-random P3HexTh. Dependence of the transition energy of the UV–vis absorption peak of the polymers on the applied pressure is shown. Original UV–vis spectra of P(Th–Ph) and ITN-copolymer are shown in Figures S27 and S28.

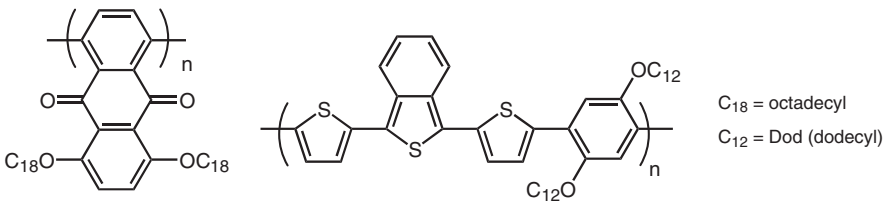


**Chart 12.** Molecular structures of the AQ-polymer[15,33c] and ITN-copolymer[27] in Figure 11B.

Ph) at 445 nm in chloroform shifts to 508 and 546 nm in the cast film of P(Th–Ph),[12b] which supports the presence of a strong electronic interaction through the $\pi$-stacking. The observed density of P(Th–Ph) (1.18 g cm$^{-3}$) agreed with density (1.18 g cm$^{-3}$) calculated from $d_1$, $d_2$, and the somewhat longer –Th–Ph– repeating length (7.8 Å) than the assumed –Th–Th– repeating length (7.7 Å; cf. Figure 5).

**Piezochromism.** Application of high pressure to $\pi$-conjugated compounds, including transition-metal complexes having $\pi$-conjugated ligands[30] and $\pi$-conjugated oligomers[31] and polymers,[15,32,33] is considered to increase electronic interaction between the compounds, and it actually causes shifts of the UV–vis absorption peaks of the compounds.[15,32,33]

Figure 11A shows the dependence of transition energy of UV–vis absorption peaks on the applied pressure for the polymers reported in this paper. For comparison, reported piezochromic data of an anthraquinone (AQ) polymer (curve f)[15,33c] and regio-random P3HexTh (curve g)[32b] prepared using $FeCl_3$ and those of a recently reported isothianaphthene (ITN) copolymer (Chart 12)[27] are shown in Figure 11B.

The piezochromic data shown in Figure 11 and other experimental results reveal the following features of the piezochromism.

(1) The $\pi$–$\pi^*$ transition energy is in the order HH-PTh$_4$ > TT-PTh$_3$ > HH-P3(C≡C–Dec)Th throughout the applied pressure. The difference in the number density of the –C≡C–Dec side chains seems to determine the order, similarly to the cases of the diffuse reflectance spectra of the polymers shown in Chart 9. For HH-PTh$_4$ and TT-PTh$_3$, reversibility of the piezochromism (returning of the UV–vis peak by releasing the pressure) was observed.

(2) For the polymers shown in Figure 11A, the $\pi$–$\pi^*$ transition energy seems to saturate at a high pressure of about 10 GPa. The decrease in the $\pi$–$\pi^*$ transition energy seems to be caused by shortening the face-to-face stacking distance $d_2$, which brings about a stronger intermolecular electronic interaction between the $\pi$-conjugated polymers. Samuelsen reported shortening of $d_2$ of regio-regular HT-P3OctTh (Oct = octyl) by about 10% at 8 GPa and that the shortening saturates at about 8 GPa.[34] Piezochromism of the AQ-polymer and ITN-copolymer is discussed below.

(3) Polythiophenes (HH-P3(C≡C–Dec)Th, TT-PTh$_3$, HH-PTh$_4$, and regio-random P3HexTh (curve (g) in Figure 11B) show an analogous shift of the UV–vis absorption peak upon the application of high pressure. A reported shift of the UV–vis peak of HT-P3HexTh up to 0.5 GPa (0.04 eV at 0.5 GPa or 0.08 eV GPa$^{-1}$)[32a] and a shift of the PL peak of HT-P3HexTh at high pressure (about 0.15 eV at 5 GPa or 0.03 eV GPa$^{-1}$)[33c] seems to be comparable to the shift of the UV–vis transition energy of polythiophenes shown in Figure 11, if one takes into account a relatively large shift per unit pressure in a region of low added pressure.

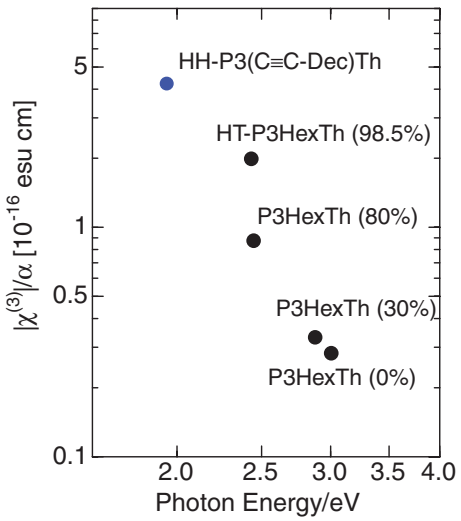


**Figure 12.** Plots of $\chi^{(3)}/\alpha$ vs. photon energy of $\pi$–$\pi^*$ transition, which is estimated from the UV–vis absorption peak;[7e] $\chi^{(3)}$ of HH-P3(C≡C–Dec)Th is from Ref. 17e. The figure in the parentheses indicates the HT-content of P3HexTh.[7f] For each polymer, the peak $\chi^{(3)}$ value is adopted.

(4) The ITN-copolymer shows a somewhat weak dependence of the UV–vis peak on the pressure. This may be due to a strong $\pi$-stacking interaction between the polymer chains even without application of high pressure. The ITN-copolymer seemed to be soluble in 1,2,4-trichlorobenzene at 140 °C, however, its GPC analysis in 1,2,4-trichlorobenzene at 140 °C was not possible,[27] suggesting that the copolymer had a strong tendency to self-assemble by inter-chain interaction. The AQ-polymer shows a stronger piezochromism and the $\pi$–$\pi^*$ transition energy of the polymer seems to continue to decrease even at pressures higher than 10 GPa. The AQ-polymer is believed to have a strongly twisted main chain due to the presence of bulky side chains, and coplanarization of its main chain at high pressures seems to explain piezochromism at pressures over 10 GPa.

**Optical Third-Order Nonlinear Susceptibility $\chi^{(3)}$.** Processable $\pi$-conjugated polymers with a large $\chi^{(3)}$ are important materials for switching light (e.g., for photocommunication systems).[35] Figure 12 shows a comparison of $\chi^{(3)}/\alpha$ ($\alpha$ = absorption coefficient) of HH-P3(C≡C–Dec)Th with those of P3HexTh's with various HT-content. All polymers in Figure 12 reasonably showed a peak $\chi^{(3)}$ at a wavelength ($\lambda^{(3)}$) of irradiated light,[17e,35] giving a correlation $\lambda^{(3)} = 3\lambda_{max}$ ($\lambda_{max}$ = wavelength of the $\pi$–$\pi^*$ transition of the polymer). The data shown in Figure 12 are based on the peak $\chi^{(3)}$. The value of $\chi^{(3)}/\alpha$ is an effective measure of third optical nonlinearity because the difference of the $\pi$ density between the samples is cancelled.

As shown in Figure 12, HH-P3(C≡C–Dec)Th has a larger $\chi^{(3)}/\alpha$ than the P3HexTh's, which is essentially attributed to a large conjugation length due to high coplanarity of HH-P3(C≡C–Dec)Th and a smaller $\pi$–$\pi^*$ transition energy of HH-P3(C≡C–Dec)Th than those of P3HexTh's. $\chi^{(3)}$ primarily increases with an increase in $\lambda_{max}$, according to equation $\chi^{(3)} \propto (\lambda_{max})^6$ or $(1/E)^6$ ($E$ = photon energy of the $\pi$–$\pi^*$ transition).[7f,35] $\chi^{(3)}$ ($3.6 \times 10^{-11}$ esu) of HH-P3(C≡C–Dec)Th is larger than those ($1.81 \times 10^{-12}$–$2.72 \times 10^{-11}$ esu[7f]) of poly(3-hexylthiophene)s.

## Conclusion

Polythiophenes with acetylenic –C≡CR (R = alkyl, phenyl, etc.) side chains have been prepared. HH-P3(C≡C–alkyl)Th, HH-$PTh_3$, TT-$PTh_3$, HH-$PTh_4$, TT-$PTh_4$, HH-P3(C≡C–Ph)Th, HH-P3(C≡C–Ph–Bu)Th, and HH-P3(C≡C–Th–Dod)Th are believed to have an intrinsically coplanar structure, and they showed a strong tendency to form a $\pi$-stacked molecular assembly. They provide basic information about the packing structure and optical data of coplanar polythiophenes in solution and/or in the solid state. P(Th–Ph) also shows a strong tendency to assemble molecularly. The polymers exhibit piezochromism, and HH-P3(C≡C–Dec)Th has a larger $\chi^{(3)}$ than P3HexTh's.

We are grateful to Professor M. Hasegawa and Dr. H. Ohtsu of Aoyama-Gakuin University and Dr. H. Kokubo and Mrs. S. Shiozaki of our laboratory for helpful discussion and experimental support. This study was partly supported by a Grant-in-Aid for Scientific Research on Priority Areas "Super-Hierarchical Structures" supported by Ministry of Education, Culture, Sports, Science and Technology, Japan.

## Supporting Information

Crystallographic data for monomers and related compounds, profiles of potential energy vs. dihedral angle of model compounds, CP/MAS solid-state $^{13}C$ NMR spectra of the polymers, optical and NMR data other than those described in the text, cyclic voltammograms of HH-P3(C≡C–Dec)Th, XRD data other than those described in the text, pictures of P(Th–Ph), UV–vis spectra of the polymers under high pressure, and synthetic data of monomers and polymers (30 pages). This material is available free of charge on the Web at http://www.csj.jp/journals/bcsj/.

## References

1 a) T. J. Skotheim, J. R. Reynolds, *Handbook of Conducting Polymers*, Third Edition, CRC Press, Boca Raton, **2007**. b) H. S. Nalwa, *Handbook of Organic Conductive Molecules and Polymers*, Vol. 2, John Wiley, Chichester, **1997**. c) W. R. Salaneck, D. L. Clark, E. J. Samuelsen, *Science and Applications of Conducting Polymers*, Adam Hilger, Bristol, **1991**. d) J. L. Brédas, R. R. Chance, *Conjugated Polymeric Materials: Opportunities in Electronics, Optoelectronics, and Molecular Electronics*, Kluwer Academic Publishers, Dordrecht, **1990**.

2 a) D. Fichou, *Handbook of Oligo- and Polythiophenes*, Wiley-VCH, Weinheim, **1999**. b) R. D. McCullough, *Adv. Mater.* **1998**, *10*, 93. c) J. Roncali, *Macromol. Rapid Commun.* **2007**, *28*, 1761. d) A. C. Grimsdale, K. Müllen, *Macromol. Rapid Commun.* **2007**, *28*, 1676. e) B. C. Thompson, J. M. J. Fréchet, *Angew. Chem., Int. Ed.* **2008**, *47*, 58. f) T. Yamamoto, *Macromol. Rapid Commun.* **2002**, *23*, 583. g) U. Scherf, E. J. W. List, *Adv. Mater.* **2002**, *14*, 477.

3 a) U. H. F. Bunz, *Chem. Rev.* **2000**, *100*, 1605. b) C. Weder, *Poly(arylene ethynylene)s*, Springer, Berlin, **2005**. c) J. M. Tour, *Acc. Chem. Res.* **2000**, *33*, 791. d) K. Yamamoto, K. Takanashi, *Polymer* **2008**, *49*, 4033.

4 a) R. D. McCullough, R. D. Lowe, *J. Chem. Soc., Chem.*

*Commun.* **1992**, 70. b) R. D. McCullough, S. Tristam-Nagle, S. P. Williams, R. D. Lowe, M. Jayaraman, *J. Am. Chem. Soc.* **1993**, *115*, 4910. c) R. D. McCullough, P. C. Ewband, R. S. Loewe, *J. Am. Chem. Soc.* **1997**, *119*, 633. d) R. Zhang, B. Li, M. C. Iovu, M. Jeffries-EL, G. Sauvé, J. Cooper, S. Jia, S. Tristam-Nagle, D. M. Smilgies, D. N. Lambeth, R. D. McCullough, T. Kowalewski, *J. Am. Chem. Soc.* **2006**, *128*, 3480. e) M. C. Iovu, E. E. Sheina, R. R. Gil, R. D. McCullough, *Macromolecules* **2005**, *38*, 8649.

5 a) T. A. Chen, R. D. Rieke, *J. Am. Chem. Soc.* **1992**, *114*, 10087. b) T.-A. Chen, X. Wu, R. D. Rieke, *J. Am. Chem. Soc.* **1995**, *117*, 233. c) A. Yokoyama, T. Yokozawa, *Macromolecules* **2007**, *40*, 4093. d) H. Mao, B. Xu, S. Holdcroft, *Macromolecules* **1993**, *26*, 1163. e) S. Amou, O. Haba, K. Shirato, T. Hayakawa, M. Ueda, K. Takeuchi, M. Asai, *J. Polym. Sci., Part A: Polym. Chem.* **1999**, *37*, 1943. f) M. R. Andersson, D. Selse, M. Berggren, H. Järvinen, T. Hjertberg, O. Inganäs, O. Wennerström, J.-E. Österholm, *Macromolecules* **1994**, *27*, 6503.

6 a) H. Sirringhaus, P. J. Brown, R. H. Friend, M. M. Nielsen, K. Beckgaard, B. M. M. Langeveld-Voss, A. J. H. Spiering, R. A. J. Janssen, E. W. Meijer, P. Herwig, D. M. de Leeuw, *Nature* **1999**, *401*, 685. b) S. Goffri, C. Müller, N. Stingelin-Stutzmann, D. W. Breiby, C. P. Radano, J. W. Andreasen, R. Thompson, R. A. J. Janssen, M. M. Nielsen, P. Smith, H. Sirringhaus, *Nat. Mater.* **2006**, *5*, 950. c) Z. Bao, A. Dodabalapur, A. J. Lovinger, *Appl. Phys. Lett.* **1996**, *69*, 4108. d) J. A. Rogers, Z. Bao, *J. Polym. Sci., Part A: Polym. Chem.* **2002**, *40*, 3327.

7 a) A. Zen, M. Saphiannikova, D. Neher, J. Grenzer, S. Grigorian, U. Pietsch, U. Asawapirom, S. Janietz, U. Scherf, I. Lieberwirth, G. Wegner, *Macromolecules* **2006**, *39*, 2162. b) R. A. Street, *Nat. Mater.* **2006**, *5*, 171. c) K. R. Amundson, B. J. Sapjeta, A. J. Lovinger, Z. Bao, *Thin Solid Films* **2002**, *414*, 143. d) R. J. Kline, D. M. DeLongchamp, D. A. Fischer, E. K. Lin, L. J. Richter, M. L. Chabinyc, M. F. Toney, M. Heeney, I. McCulloch, *Macromolecules* **2007**, *40*, 7960. e) T. Yamamoto, D. Komarudin, M. Arai, B.-L. Lee, H. Suganuma, N. Asakawa, Y. Inoue, K. Kubota, S. Sasaki, T. Fukuda, H. Matsuda, *J. Am. Chem. Soc.* **1998**, *120*, 2047. f) H. Kishida, K. Hirota, T. Wakabayashi, H. Okamoto, H. Kokubo, T. Yamamoto, *Appl. Phys. Lett.* **2005**, *87*, 121902. g) P. Gangopadhyay, R. Voorakaranam, A. Lopez-Santiago, S. Foerier, J. Thomas, R. A. Norwood, A. Persoons, N. Peyghambarian, *J. Phys. Chem. C* **2008**, *112*, 8032. h) Density of the polymer was measured by a sink and float method. Some of the polymers were partly soluble in the liquid used for the sink and float method.

8 a) M. C. Gallazzi, L. Castellani, R. A. Marin, G. Zerbi, *J. Polym. Sci., Part A: Polym. Chem.* **1993**, *31*, 3339. b) H. Kokubo, T. Yamamoto, *Macromol. Chem. Phys.* **2001**, *202*, 1031. c) H. Kokubo, T. Sato, T. Yamamoto, *Macromolecules* **2006**, *39*, 3959.

9 a) I. McCulloch, M. Heeney, C. Bailey, K. Genevicius, I. MacDonald, M. Shkunov, D. Sparrowe, S. Tierney, R. Wagner, W. Zhang, M. L. Chabinyc, R. J. Kline, M. D. McGehee, M. F. Toney, *Nat. Mater.* **2006**, *5*, 328. b) J. D. Yuen, A. S. Dhoot, E. B. Namdas, N. E. Coates, M. Heeney, I. McCulloch, D. Moses, A. J. Heeger, *J. Am. Chem. Soc.* **2007**, *129*, 14367. c) B. H. Hamadani, D. J. Gundlach, I. McCulloch, M. Heeney, *Appl. Phys. Lett.* **2007**, *91*, 243512. d) H. Ohkita, S. Cook, Y. Astuti, W. Duffy, S. Tierney, W. Zhang, M. Heeney, I. McCulloch, J. Nelson, D. D. C. Bradley, J. R. Durrant, *J. Am. Chem. Soc.* **2008**, *130*, 3030.

10 a) Y. Zhu, R. D. Champion, S. A. Jenekhe, *Macromolecules* **2006**, *39*, 8712. b) F. Wang, M.-Y. Han, K. Y. Mya, Y. Wang, Y.-H. Lai, *J. Am. Chem. Soc.* **2005**, *127*, 10350. c) H.-F. Lu, H. S. O. Chan, S.-C. Ng, *Macromolecules* **2003**, *36*, 1543. d) T. Yasuda, Y. Sakai, S. Aramaki, T. Yamamoto, *Chem. Mater.* **2005**, *17*, 6060. e) L. M. Campos, A. Tontcheva, S. Günes, G. Sonmez, H. Neugebauer, N. S. Sariciftci, F. Wudl, *Chem. Mater.* **2005**, *17*, 4031.

11 a) B. C. Thompson, Y.-G. Kim, T. D. McCarley, J. R. Reynolds, *J. Am. Chem. Soc.* **2006**, *128*, 12714. b) M. J. Panzer, C. D. Frisbie, *J. Am. Chem. Soc.* **2007**, *129*, 6599. c) B. S. Ong, Y. Wu, P. Liu, S. Gardner, *Adv. Mater.* **2005**, *17*, 1141. d) A. Herland, K. P. R. Nilsson, J. D. M. Olsson, P. Hammarström, P. Konradsson, O. Inganäs, *J. Am. Chem. Soc.* **2005**, *127*, 2317. e) J. Liu, R. Zhang, G. Sauvé, T. Kowalewski, R. D. McCullough, *J. Am. Chem. Soc.* **2008**, *130*, 13167.

12 a) T. Sato, Z. Cai, T. Shiono, T. Yamamoto, *Polymer* **2006**, *47*, 37. b) T. Sato, H. Kokubo, H. Fukumoto, T. Yamamoto, *Bull. Chem. Soc. Jpn.* **2005**, *78*, 1368.

13 a) Y. Li, G. Vamvounis, S. Holdcroft, *Macromolecules* **2002**, *35*, 6900. b) T. Yamamoto, A. Mahmut, M. Abe, S. Kuroda, T. Imase, S. Sasaki, *J. Polym. Sci., Part B: Polym. Phys.* **2005**, *43*, 2219. c) R. Yamashita, T.-A. Koizumi, S. Sasaki, T. Yamamoto, *Polym. J.* **2007**, *39*, 1202.

14 a) T. Yamazaki, Y. Murata, K. Komatsu, K. Furukawa, M. Morita, N. Maruyama, T. Yamao, S. Fujita, *Org. Lett.* **2004**, *6*, 4865. b) B. Xu, M. Lu, J. Kang, D. Wang, J. Brown, Z. Peng, *Chem. Mater.* **2005**, *17*, 2841.

15 T. Yamamoto, Y. Muramatsu, B.-L. Lee, H. Kokubo, S. Sasaki, M. Hasegawa, T. Yagi, K. Kubota, *Chem. Mater.* **2003**, *15*, 4384.

16 a) V. N. Kuznetsov, N. Serpone, *J. Phys. Chem. C* **2007**, *111*, 15277. b) P. Kubelka, F. Munk, *Z. Tech. Phys.* **1931**, *12*, 593.

17 a) J. K. Stille, *Angew. Chem., Int. Ed. Engl.* **1986**, *25*, 508. b) Z. Bao, W. K. Chan, L. Yu, *J. Am. Chem. Soc.* **1995**, *117*, 12426. c) J. Xu, S. C. Ng, H. S. O. Chan, *Tetrahedron Lett.* **2001**, *42*, 5327. d) A. Izumi, R. Nomura, T. Masuda, *Macromolecules* **2000**, *33*, 8918. e) T. Sato, H. Kishida, A. Nakamura, T. Fukuda, T. Yamamoto, *Synth. Met.* **2007**, *157*, 318. f) T. Sato, T. Yagi, H. Tajima, T. Fukuda, T. Yamamoto, *React. Funct. Polym.* **2008**, *68*, 369. A side view of alkyl chain packing proposed in this paper and Ref. 17g is misleading and is amended in Figure 5. g) T. Yamamoto, T. Sato, *Jpn. J. Appl. Phys.* **2006**, *45*, L301.

18 CP/MAS solid-state $^{13}$C NMR spectrum of HH-P3(C≡C–Bu)Th also showed sharp Th- and –C≡C– carbon signals; the –C≡C– carbon signals appeared at $\delta$ 78.0 and 100.9. In contrast, CP/MAS solid-state $^{13}$C NMR spectrum of regio-random P3(C≡C–Bu)Th, prepared from Br–Th(C≡C–Bu)–Br using $Pd(PPh_3)_4$ and $Me_3SnSnMe_3$ (cf. eq 2), showed broad Th- and –C≡C– carbon signals, similar to the case of regio-random P3HexTh shown in Figure 2b.

19 a) J.-F. Chang, B. Sun, D. W. Breiby, M. M. Nielsen, T. I. Sölling, M. Giles, I. McCulloch, H. Sirringhaus, *Chem. Mater.* **2004**, *16*, 4772. b) Q. Fang, A. Tanimoto, T. Yamamoto, *Synth. Met.* **2005**, *150*, 73.

20 a) J. T. Lopez-Navarrete, G. Zerbi, *J. Chem. Phys.* **1991**, *94*, 957. b) G. Zerbi, B. Chierichetti, O. Ingänas, *J. Chem. Phys.* **1991**, *94*, 4637.

21 UV–vis diffuse reflectance spectra of powdery HH-P3(C≡C–Dec)Th, P(Th–Ph), and HT-P3HexTh are shown in Figures S20a, S20g, and S20h, respectively. Comparison of these spectra with UV–vis spectra of cast films of HH-P3(C≡C–Dec)Th, P(Th–Ph),[12b] and HT-P3HexTh[1–3] indicates that the UV–vis diffuse reflectance spectrum gives the $\lambda_{max}$ peak at a wavelength somewhat longer by about 20 nm than that of the polymer film.

22 a) D. Fichou, C. Ziegler, In Ref. 2a. X-ray crystallographic data of oligothiophenes suggest that the –Th–Th– repeating distance (e.g., cf. Figure 5a) in polythiophenes is in the range of 7.5–7.8 Å. b) K. E. Aasmundtveit, E. J. Samuelsen, L. A. A. Pettersson, O. Inganäs, T. Johansson, R. Feidenhaus'l, *Synth. Met.* **1999**, *101*, 561. A repeating length of 7.8 Å was reported for two repeating thiophene units in p-doped poly(ethylenedioxythiophene). c) H. W. S. Hsieh, B. Post, H. Morawetz, *J. Polym. Sci.: Polym. Phys. Ed.* **1976**, *14*, 1241. d) E. F. Jordan, Jr., D. W. Feldeisen, A. N. Wrigley, *J. Polym. Sci., Part A: Polym. Chem.* **1971**, *9*, 1835. e) I.-C. Lin, O.-A. von Lilienfeld, M. D. Coutinho-Neto, I. Tavernelli, U. Rothlisberger, *J. Phys. Chem. B* **2007**, *111*, 14346. f) C. K. Mathews, van K. E. Holde, *Biochemistry*, Cummings Publishing, Redwood City, **1990**, p. 103. g) C. F. Matta, N. Castillo, R. J. Boyd, *J. Phys. Chem. B* **2006**, *110*, 563. h) M. Egli, V. Tereshko, G. N. Mushudov, R. Sanishvili, X. Liu, F. D. Lewis, *J. Am. Chem. Soc.* **2003**, *125*, 10842. i) S. Nakano, Y. Uotani, S. Nakashima, Y. Anno, M. Fujii, N. Sugimoto, *J. Am. Chem. Soc.* **2003**, *125*, 8086.

23 $\rho_{calcd} = (493$ (molecular weight of the repeating unit of HH-P3(C≡C–Dec)Th))/$(7.7 \times 10^{-8} \times 3.8 \times 10^{-8} \times 24 \times 10^{-8} \times 6.0 \times 10^{23}) = 1.17\,g\,cm^{-3}$; for the lengths, see Figure 5. The observed density of polymer is usually somewhat smaller than the calculated density due to the presence of some amorphous parts in the polymer solid.

24 The cast film or the powder of HH-P3(C≡C–Dec)Th was rubbed by hand with a spatula. In view of the contact area of the spatula and the power applied by the hand, the applied pressure was roughly estimated at about 30 MPa.

25 M. Brinkmann, P. Rannou, *Adv. Funct. Mater.* **2007**, *17*, 101.

26 a) T. Yamamoto, H. Kokubo, *Mol. Cryst. Liq. Cryst.* **2002**, *381*, 113. b) T. Yamamoto, H. Kokubo, *Chem. Lett.* **1999**, 1295. c) T. Yamamoto, H. Kokubo, *Electrochim. Acta* **2005**, *50*, 1453.

27 T. Yamamoto, H. Ootsuka, T. Iijima, *Macromol. Rapid Commun.* **2007**, *28*, 1786.

28 a) T. Yamamoto, K. Shiraishi, M. Abla, I. Yamaguchi, L. B. Groenendaal, *Polymer* **2002**, *43*, 711. b) Y. Lei, H. Oohata, S. Kuroda, S. Sasaki, T. Yamamoto, *Synth. Met.* **2005**, *149*, 211.

29 T. Yamamoto, *Bull. Chem. Soc. Jpn.* **1999**, *72*, 621.

30 a) I. Shirotani, A. Kawamura, K. Suzuki, W. Utsumi, T. Yagi, *Bull. Chem. Soc. Jpn.* **1991**, *64*, 1607. b) I. Shirotani, K. Suzuki, T. Suzuki, T. Yagi, *Bull. Chem. Soc. Jpn.* **1992**, *65*, 1078.

31 J. Kunzelman, M. Kinami, B. R. Crenshaw, J. D. Protasiewicz, C. Weder, *Adv. Mater.* **2008**, *20*, 119.

32 a) T. Kaniowski, S. Niziol, J. Sanetra, M. Trznadel, A. Proń, *Synth. Met.* **1998**, *94*, 111. b) K. Iwasaki, H. Fujimoto, S. Matsuzaki, *Synth. Met.* **1994**, *63*, 101. c) K. Yoshino, K. Nakao, M. Onoda, *Jpn. J. Appl. Phys.* **1989**, *28*, L323. d) K. Yoshino, S. Nakajima, M. Onoda, R. Sugimoto, *Synth. Met.* **1989**, *28*, 349.

33 a) M. Leclerc, *Adv. Mater.* **1999**, *11*, 1491. b) R. W. Carpick, D. Y. Sasaki, M. S. Marcus, M. A. Eriksson, A. R. Burns, *J. Phys.: Condens. Matter* **2004**, *16*, R679. c) Y. Muramatsu, T. Yamamoto, M. Hasegawa, T. Yagi, H. Koinuma, *Polymer* **2001**, *42*, 6673.

34 E. J. Samuelsen, J. Mårdalen, O. R. Konestabo, M. Hanfland, M. Lorenzen, *Synth. Met.* **1999**, *101*, 98.

35 a) W. J. Blau, in *Electronic Properties of Polymers (Springer Series in Solid-State Sciences)*, ed. by H. Kuzmany, M. Mehring, S. Roth, Springer, Berlin, **1992**, Vol. 107. b) C. Sauteret, J.-P. Hermann, R. Frey, F. Pradère, J. Ducuing, R. H. Baughman, R. R. Chance, *Phys. Rev. Lett.* **1976**, *36*, 956. c) H. Kishida, K. Hirota, H. Okamoto, H. Kokubo, T. Yamamoto, *Appl. Phys. Lett.* **2008**, *92*, 033309. d) T. Yamamoto, Z.-H. Zhou, T. Kanbara, M. Shimura, K. Kizu, T. Maruyama, Y. Nakamura, T. Fukuda, B.-L. Lee, N. Ooba, S. Tomaru, T. Kurihara, T. Kaino, K. Kubota, S. Sasaki, *J. Am. Chem. Soc.* **1996**, *118*, 10389. e) T. Yamamoto, B.-L. Lee, H. Kokubo, H. Kishida, T. Hirota, T. Wakabayashi, H. Okamoto, *Macromol. Rapid Commun.* **2003**, *24*, 440.